JREE: Vol. 6, No. 3, (Summer 2019) 16-23

Journal of Renewable Energy and Environment

Research Article

Journal Homepage: www.jree.ir

Thermodynamic Based Working Fluid Selection for High-Temperature Waste Heat Recovery of a Turbocharged Diesel Engine Using Organic Rankine Cycle

Amin Habibzadeh[a,b*], Samad Jafarmadar[b]

[a] *Young Researchers Club, Urmia Branch, Islamic Azad University, Urmia, Iran.*
[b] *Department of Mechanical Engineering, Faculty of Engineering, Urmia University, Urmia, Iran.*

PAPER INFO

Paper history:
Received 12 September 2019
Accepted in revised form 21 December 2019

Keywords:
Organic Rankine Cycle
Waste-Heat Recovery
Diesel Engines
Working Fluids
Energetic and Exergetic Analysis

ABSTRACT

A considerable amount of waste heat is produced by internal combustion engines. Bottoming cycle application of Organic Rankine Cycles (ORC) is one of the promising technologies that recuperates the waste heat of engines. A lot of engine waste heat is released into the environment. There are a lot of working fluids that can be applied in these cycles. As the engine waste heat temperature is extremely high, finding a suitable working fluid, which operates properly in the combined cycle, is challenging. In this paper, the thermodynamic analysis of ten working fluids including cyclohexane, HFE7000, HFE7100, n-hexane, n-pentane, R11, R123, R134a, R141b, and R245fa is conducted to observe the influence of different parameters on the system performance and introduce the most appropriate working fluid. Results indicated that, in the studied ranges, R134a had the best performances since (a) its thermal and exergy efficiencies were 17.39 % and 17.34 %, respectively; (b) the thermal efficiency of the engine increased by 9 %, and the net power of the system reached 7.5 kW. Furthermore, there was about 9 % reduction in fuel consumption. On the other hand, among the studied working fluids, cyclohexane operates as the least suitable one by possessing the minimum amounts.

1. INTRODUCTION

Fossil fuels are the source of most energies. The rising prices of fossil fuel and pollution problems caused by burning fossil fuels have necessitated researchers to look for and study novel sources such as wind, geothermal, solar, and different types of waste heat [1]. A lot of thermal energy from different processes is wasted into the environment [2-4]. The waste heat from engines (internal combustion engines) has received researchers' attention since these engines in their best-operating conditions convert 40-45 % of the fuel energy into the useful power, and the rest is lost as the exhaust gas and cooling system. The waste heat released from these engines is classified into low-to-medium grade energy sources and can be reused by applying a waste heat recovery (WHR) system. Among the bottoming cycles coupled with the engines, Organic Rankine cycle (ORC) is one of the most premier technologies when considering its high thermal efficiency, simplicity, and compatibility with a vast range of heat [5]. Patel and Doyle [6] were among the first researchers that studied a combination of ORC and the exhaust gas of a diesel engine. After that, different researchers have investigated ORC-WHR cycles. In an outstanding study by Vaja and Gambarotta [7], the thermodynamic analysis of different working fluids was considered in order to match a vapor cycle with an internal combustion engine. Their analysis showed that a 12 % rise in the total efficiency could be achieved compared to the engine without using ORC cycle. Lu et al. [8] reported the generation of 1 kW power in a 6.5 kW engine by applying ORC to recover exhaust energy in a diesel engine. Preheat and two-stage configurations were introduced by Tahani et al. [9] to apply the waste heat recovery system in a 12-liter diesel engine. Among the studied working fluids, R123 enjoyed the highest performance in both configurations and fuel consumption decrease. A novel Organic Rankine Cycle system was proposed by Panesar [10] to convert the waste heat into viable power in the long-haul trucks. The results showed that, by installing this system, the system power increased by 20 % and the brake thermal efficiency raised by 1.8 %. Yu et al. [11] studied the application of ORC for a diesel engine to reuse waste heat from the exhaust gas and jacket water by using R245fa. The results depicted that 75 % of exhaust gas and 9.5 % of jacket water could be recovered. Moreover, the mentioned system generated higher exergy and thermal efficiencies. A CNG engine-ORC with the IHE combined system was designed by Song et al. [12] to improve the electric efficiency. By applying the WHR system, the net power, electric efficiency, and thermal efficiency of the cycle increased, while the BSFC decreased. Song and Gu [13] examined a mixture of a hydrocarbon and a retardant used in an ORC-WHR system. According to the first and second laws of analysis, cyclohexane/R141b (0.5/0.5), compared to pure cyclohexane, showed a 13.3 % increase in net power output. Shu et al. [14] surveyed the usage of alkanes as the working fluids of the combined system of a diesel engine and bottoming ORC. By considering six indicators including thermal efficiency, exergy destruction factor, turbine size parameter, total exergy destruction rate, turbine volume flow ratio, and net power output per unit mass flow rate of exhaust, it was proved that cyclic Alkanes, Cyclohexane, and Cyclopentane were the most suitable working fluids.

In a study by Kim et al. [15], a novel single-loop ORC system was introduced by adding an LT recuperator to fully utilize the residual heat. By comparing the performances of conventional systems on a gasoline passenger car to recover

*Corresponding Author's Email: a.habibzadeh@urmia.ac.ir (A. Habibzadeh)

waste heat, they showed that the system output power could be increased by up to 20 % when using a novel single-loop system.

In spite of numerous studies on ORC-WHR systems, a cycle that recovers both low-temperature source (engine coolant) and high-temperature source (exhaust gas) in the engine at the same time is very scarce. Therefore, this study proposes implementing a single-loop ORC system for a diesel engine waste heat recovery system by applying different working fluids and identifying the most suitable one by taking into consideration different aspects such as the first and second laws of analysis.

Table 1. The main parameters of the 1004-4T diesel engine.

Parameter	Unit	Value
Power output	kW	71.2
Rotation speed	r/min	2000
Torque	Nm	340
Exhaust heat temperature	K	823.15
Mass flow rate of engine exhaust gas	kg/h	18.9
Fuel consumption	kg/h	15.6

2. WASTE HEAT RECOVERY SYSTEM MODELING

In the present study, a four-cylinder, turbo-charged diesel engine is applied as a topping system, and the main parameters of the diesel engine are listed in Table 1. For recovering waste heat, Organic Rankine Cycle is defined as the bottoming cycle. A schematic diagram of the cycle and T-S diagram is shown in Figures. 1 and 2. The ORC system consists of a pump, two LT and HT recuperators, a preheater, an evaporator, an expander, and a condenser. The whole system operates as follows:

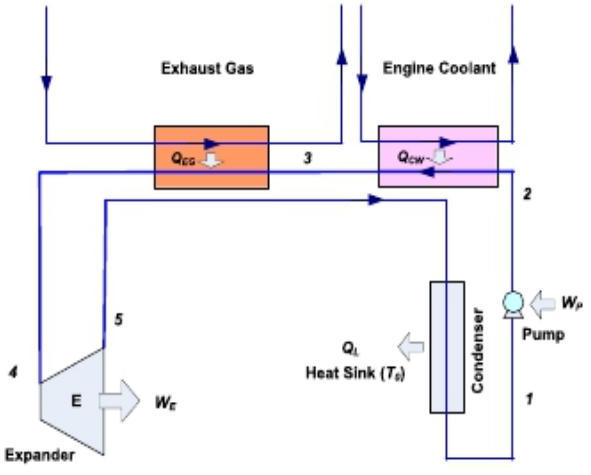

Figure 1. Schematic of a single-loop ORC system combined with a diesel engine.

The high-temperature waste heat of the diesel engine can be recovered via bottoming an Organic Rankine Cycle. The exhaust gas can exchange heat in the evaporator with the working fluid before being released into the atmosphere. In the ORC process, the working fluid is pumped (1-2) in an isentropic process. As the jacket cooling water temperature is low, it is appropriate for preheating. Therefore, the preheater recovers the heat from the jacket water cooler, while the evaporator recovers the heat from the exhaust energy in an isobaric heat transfer process (3-4 and 5-6). In an isentropic expansion process inside the expander, the fluid is expanded in the expander to produce mechanical power (6-7). Passing the expander, the working fluid enters the condenser where it condenses into saturated liquid in an isobaric heat transfer process (9-1). In order to reuse the residual heat of working fluid leaving the expander and preheat the working fluid, two HT and LT recuperators are added (2-3 and 4-5).

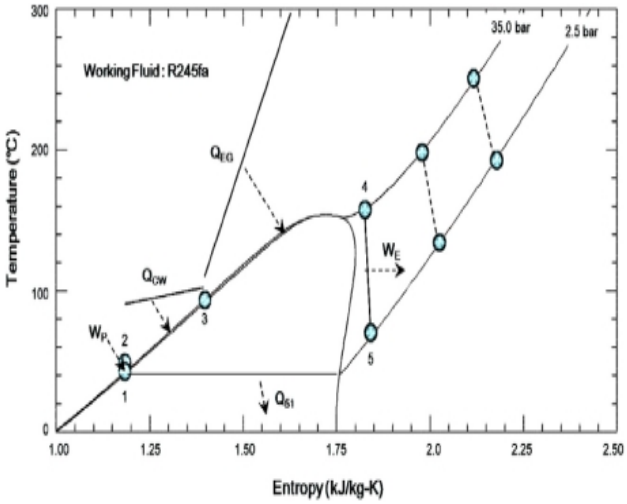

Figure 2. T-s diagram of the ORC system.

The main assumptions concerning the simulation of the combined cycle are summarized in Table 2.

To simplify the simulation of the proposed cycle, the following assumptions are also made:

(1) The cycle operates in a steady state.
(2) The kinetic and potential energies and the heat and friction losses are neglected.
(3) No pressure drops in the pipes, condenser, and evaporator.
(4) The fluid leaving the condenser is saturated.

Table 2. The main assumptions of the cycle.

Environment temperature (K)	293.15
Environment pressure (atm)	1
Condensation temperature (K)	308.15
Inlet temperature of cooling water (K)	343.2
Expansion ratio of the expander	3.5
Pump isentropic efficiency (%)	80
Expander isentropic efficiency (%)	70
Recuperator effectiveness (%)	80
Waste heat initial temperature (K)	823.15

3. WORKING FLUID SELECTION

Generally, choosing an appropriate working fluid is one of the most important factors in designing the cycle. There are some factors that a working fluid should satisfy such as Non-fouling, non-corrosiveness, non-toxicity, and non-flammability. In order to consider the environmental effects, three parameters including ozone depletion potential (ODP), global warming potential (GWP), and the atmospheric lifetime

(ALT) should be taken into consideration. ODP is the potential of a working fluid to destroy the ozone layer.

Table 3. Thermodynamic properties of working fluids.

Name	T_{crit} (^{o}c)	P_{crit} (kPa)	M (g/mol)	ODP	GWP (100yr)
Cyclohexane	280.49	4075	84.161	0	very low
HEF7000	165	2480	200	0	370
HEF7100	195.3	2330	250	0	320
N-Hexane	234.67	3034	86.175	N/A	N/A
N-Pentane	196.5	3364	72.149	N/A	5
R11	198	4408	137.37	1	4600
R123	183.7	3660	152.93	0.02	77
R134a	101	4059	102.03	0.055	1430
R141b	204.4	4460	116.95	0.086	725
R245fa	154	36500	134.05	0	1030

GWP is the potential of a working fluid to cause global warming. ALT is the amount of time that greenhouse gases need to leave the atmosphere. In general, organic working fluids are divided into dry, isentropic, and wet categories. The properties of the considered fluids are shown in Table 3.

4. THERMODYNAMIC ANALYSIS

4.1. Energy analysis

Based on the first law of thermodynamics, the behavior of different working fluids under different working conditions can be described as follows:

For the pump:

$$\dot{W}_p = \dot{m}_{wf}\,(h_2 - h_1) \tag{1}$$

$$\eta_p = \frac{h_{2s} - h_1}{h_2 - h_1} \tag{2}$$

For condenser:

$$\dot{Q}_{con} = \dot{m}_{wf}\,(h_9 - h_1) = \dot{m}_{cw}\,(h_{cw,out} - h_{cw,in}) \tag{3}$$

For the evaporator:

$$\dot{Q}_{eva} = \dot{m}_{wf}\,(h_6 - h_5) = \dot{m}_g(h_{g,in} - h_{g,out}) \tag{4}$$

For the expander:

$$\dot{W}_{exp} = \dot{m}_{wf}\,(h_7 - h_6) \tag{5}$$

The expander expansion ratio is defined as follows:

$$\beta = \frac{P_2}{P_1} \tag{6}$$

For the preheater:

$$\dot{Q}_{ph} = \dot{m}_{wf}\,(h_4 - h_3) = \dot{m}_{jw}\,(h_{jw,in} - h_{jw,out}) \tag{7}$$

The expander isentropic efficiency is:

$$\eta_{exp} = \frac{h_6 - h_7}{h_6 - h_{7s}} \tag{8}$$

For the recuperators:

$$\dot{Q}_{HT} = \dot{m}_{wf}\,(h_8 - h_7) = \dot{m}_{wf}\,(h_4 - h_5) \tag{9}$$

$$\dot{Q}_{LT} = \dot{m}_{wf}\,(h_9 - h_8) = \dot{m}_{wf}\,(h_2 - h_3) \tag{10}$$

The cycle net power output is:

$$\dot{W}_{net} = \dot{W}_{exp} - \dot{W}_p \tag{11}$$

The thermal efficiency of the combined cycle is as follows:

$$\eta_{th} = \frac{\dot{W}_{net}}{\dot{m}_g\,(h_{in} - h_{out}) + \dot{m}_{jw}\,(h_{in} - h_{out})} \tag{12}$$

4.2. Exergy analysis

Since energy efficiencies can not inform how close the performance of the system to the ideality is, the exergy analysis is required. Exergy is defined as the maximum reversible work since the system operates in an equilibrium state and depicts the inefficiencies of the system.

The exergy destruction rate for a steady state is:

$$\dot{E}_D = \sum(\dot{m}\psi)_{in} - \sum(\dot{m}\psi)_{out} + \left[\sum\left(\dot{Q}\left(1 - \frac{T_0}{T}\right)\right)_{in} + \sum\left(\dot{Q}\left(1 - \frac{T_0}{T}\right)\right)_{out}\right] \pm \sum\dot{W} \tag{13}$$

where $\dot{Q}$ is the heat transfer rate, $\dot{W}$ is the work rate, $\dot{m}$ is the mass flow rate, and T_0 is the environmental temperature.

The irreversibility of each component is expressed as follows:

$$\dot{I}_i = \sum\dot{E}_{in} - \sum\dot{E}_{out} - \dot{W}_i \tag{14}$$

Irreversibility equations for the component of the cycle are as follows:

$$I_p = \dot{m}_{wf} \times T_0 \times (s_2 - s_1) \tag{15}$$

$$I_{eva} = \dot{m}_{wf} \times T_0 \times [(s_6 - s_5) - (\frac{h_6 - h_5}{T_{m,eva}})] \tag{16}$$

$T_{m,eva}$ is the mean temperature during the evaporation process.

$$T_{m,eva} = \frac{(T_{g,in} - T_{g,out})}{\ln\frac{T_{g,in}}{T_{g,out}}} \tag{17}$$

$$I_{exp} = \dot{m}_{wf} \times T_0 \times (s_7 - s_6) \tag{18}$$

$$I_{con} = \dot{m}_{wf} \times T_0 \times [(s_1 - s_9) - (\frac{h_1 - h_9}{T_{m,con}})] \tag{19}$$

$$T_{m,con} = \frac{(T_{cw,in} - T_{cw,out})}{\ln\frac{T_{cw,in}}{T_{cw,out}}} \tag{20}$$

$$I_{ph} = \dot{m}_{wf} \times T_0 \times [(s_4 - s_3) - (\frac{h_4 - h_3}{T_{m,ph}})] \tag{21}$$

$$T_{m,ph} = \frac{(T_{jw,in} - T_{jw,out})}{\ln\frac{T_{jw,in}}{T_{jw,out}}} \tag{22}$$

$$I_{LT,r} = \dot{m}_{wf} \times T_0 \times (s_8 - s_9) + \dot{m}_{wf} \times T_0 \times (s_3 - s_2) \tag{23}$$

$$I_{HT,r} = \dot{m}_{wf} \times T_0 \times (s_7 - s_8) + \dot{m}_{wf} \times T_0 \times (s_5 - s_4) \tag{24}$$

The total exergy destruction is given by:

$$I_{tot} = I_p + I_{eva} + I_{exp} + I_{con} + I_{pre} + I_{HT,r} + I_{LT,r} \tag{25}$$

The exhaust gas exergy loss is:

$$I_g = \dot{m}_g \times C_g \times (T_{g,out} - T_0) + T_0 \times \ln\frac{T_{g,out}}{T_0} \quad (26)$$

The cycle's exergy efficiency is expressed as follows:

$$\eta_{ex} = \frac{\dot{W}_{net}}{[\dot{m}_g (h_{in} - h_{out}) - T_0 \times \ln\frac{T_{g,in}}{T_0}] + [\dot{m}_{jw} (h_{in} - h_{out}) - T_0 \times \ln\frac{T_{jw,in}}{T_{jw,out}}]} \quad (27)$$

Exergy destruction factor is calculated as follows:

$$EDF = \frac{I_{tot}}{\dot{W}_{net}} \quad (28)$$

ORC-WHR cycle usage causes an increase in the thermal efficiency of the engine. The engine thermal efficiency can be calculated as follows:

$$\eta_{th,eng} = \frac{P_{eng}}{\dot{m}_{fuel} \times LHV} \quad (29)$$

Moreover, when the engine is bottomed with an ORC, the engine thermal efficiency becomes:

$$\eta_{th,eng,ORC} = \frac{P_{eng} + \dot{W}_{net}}{\dot{m}_{fuel} \times LHV} \quad (30)$$

Lower heating value (LHV) of the fuel is considered 43 MJ/kg.

In order to show the fuel reduction percentage of the cycle, the following equation can be used as follows:

$$FRP = [1 - \frac{\eta_{th,eng}}{\eta_{th,eng} - ORC}] \times 100 \quad (31)$$

5. RESULTS AND DISCUSSION

A program based on the above analysis using EES software [16] has been developed to simulate the ORC-WHR cycle. In order to validate the simulation, the obtained results have been compared with Vaja and Gambarotta [7] and shu et al. [14] under the same conditions. The comparison is presented in Table 4 and shows very good agreement between the results. Therefore, the model is validated.

Table 4. Present numerical model validation with the previously published data.

Parameter	Working fluid	Present	Vaja and Gambarotta [7]	Shu et al. [14]
$\dot{W}_{net}$ (kW)	Benzene	391.36	351.2	394.3
	R11	289.4	292.4	290.3
	R134a	147.1	148.7	147.5
Mass flow rate (kg/s)	Benzene	2.731	2.743	2.737
	R11	7.471	7.514	7.487
	R134a	9.025	9.013	8.966

Based on the assumptions in Table 3, the detailed data of the analyzed cycles for 10 different working fluids are listed in Table 5.

Table 5. The detailed data of the analyzed cycles for 10 different working fluids.

	$\dot{W}_{net}$	I_{tot}	EDF	$\eta_{th,eng}$	$\eta_{th,eng,ORC}$	η_{ex}	η_{th}	FRP
Unit	kW	kW	-	%	%	%	%	%
Cyclohexane	4.902	15.748	0.0053	38.21	40.84	12.06	12.07	6.441
HFE7000	5.377	19.024	0.0059	38.21	41.1	13.23	13.25	7.021
HFE7100	4.918	19.654	0.0058	38.21	40.85	12.1	12.11	6.461
N-Hexane	5.047	17.197	0.0055	38.21	40.92	12.42	12.43	6.619
N-Pentane	5.47	17.695	0.0059	38.21	41.29	14.13	14.15	7.461
R11	6.142	16.152	0.006	38.21	41.51	15.12	15.15	7.942
R123	5.922	17.280	0.0057	38.21	41.39	14.57	14.6	7.679
R134a	7.048	20.512	0.006	38.21	41.99	17.34	17.39	9.007

By studying the cycle exactly, the following conclusions can be made:

1- Net power of the system, which is one of the main parameters in evaluating the efficiency of the cycle, is maximum for R134a and minimum for Cyclohexane.
2- Coupling the engine with the ORC cycle leads to an increase in thermal efficiency. According to the results, R134a and cyclohexane have the maximum and minimum amounts, respectively.
3- R134a has the highest thermal and exergy efficiency in the studied range.
4- Fuel reduction percentage is a factor to show how much the cycle helps reduce the fuel consumption. By using R134a, the cycle uses 9% lower fuel, which is a high number.

By taking into consideration the studied results, R134a is the best working fluid among the studied ones from the first and second laws of the thermodynamic view. The results of varying parameters and their effects on the efficiency of the working fluids are studied in the following sections.

5.1. Effect of the exhaust gas temperature

Figures 3 and 4 show the amounts of the thermal efficiency for different working fluids under the conditions of exhaust gas temperature varying from 700-850 K. According to the graphs, for all proposed working fluids, the thermal and exergy efficiencies of the cycle decrease when the exhaust gas temperature increases. Since the exhaust temperature has no effect on the net power of the cycle, the reduction of the energy and exergy efficiencies occurs due to the use of the heat transfer change in the evaporator. Among the studied fluids, R134a possesses the maximum amount, while Cyclohexane has the minimum quantity.

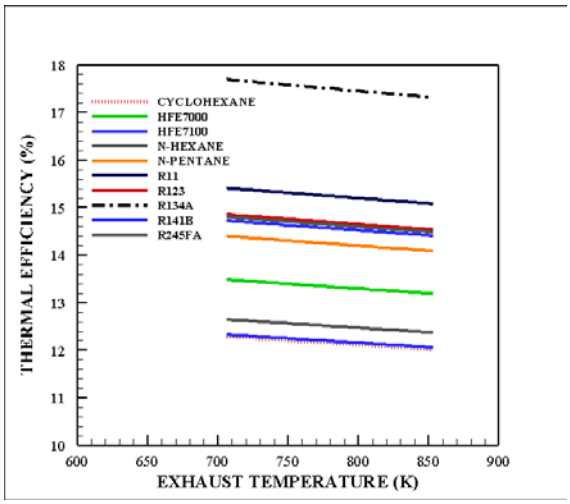

Figure 3. Effect of the exhaust temperature on the thermal efficiency.

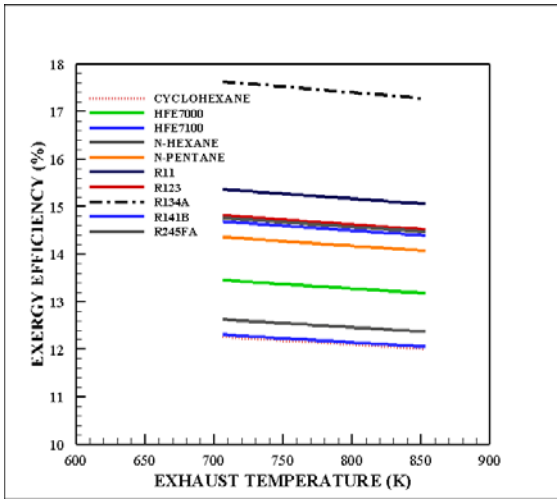

Figure 4. Effect of the exhaust temperature on the exergy efficiency.

5.2. Effect of the condenser temperature

According to Figure 5, the rise of condenser temperature causes an increase in the exergy total loss of the system. As the temperature rises, a significant increase in the exergy destruction occurs.

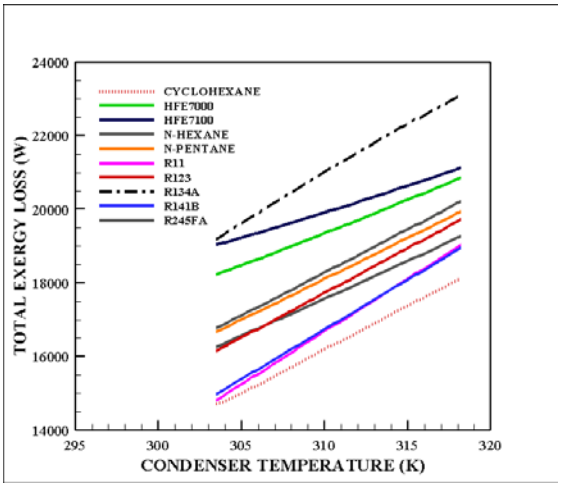

Figure 5. Effect of the condenser's temperature on the total exergy loss.

From Figures 6 and 7, it is apparent that the thermal and exergy efficiencies decrease with an increase in the condenser's temperature. By increasing the condenser's temperature, the work of the expander and pump decreases and increases, respectively, leading to a decrease in the efficiencies of the first and second laws. R134a has the highest amount, whereas Cyclohexane has the lowest.

Figure 8 depicts the effect of the condenser's temperature on the fuel reduction percentage. According to the graphs, FRP of the cycle reduces as the condenser temperature increases. The reason for this occurrence is the reduction of the total work of the cycle by the changing temperature. In the studied range, R11 and Cyclohexane have the maximum and minimum amounts of FRP, respectively.

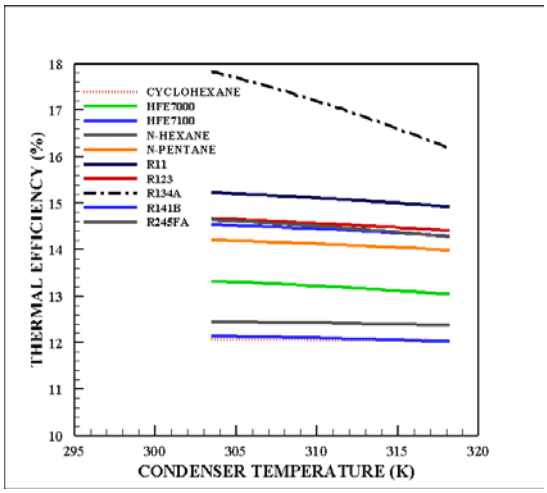

Figure 6. Effect of the condenser's temperature on the thermal efficiency.

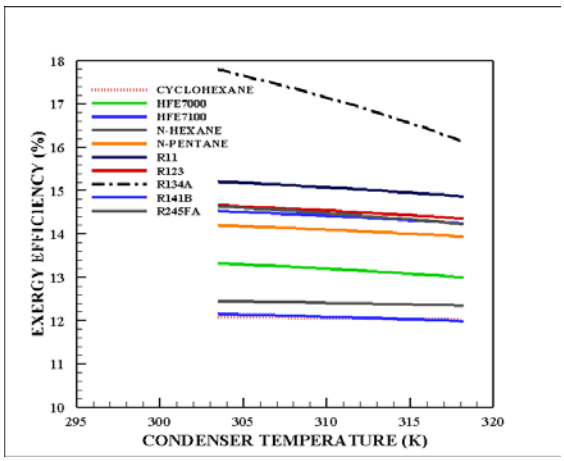

Figure 7. Effect of the condenser's temperature on the exergy efficiency.

5.3. Effect of the expander temperature

Figures 9 and 10 indicate that by increasing the expander's inlet temperature, both thermal and exergy efficiencies increase greatly. The reason for this rise is that increasing the expander's inlet temperature leads to the higher outlet power of the expander, resulting in the higher net power of the cycle. Among the studied working fluids, R134a has the maximum efficiency, while HFE7100 has the minimum one.

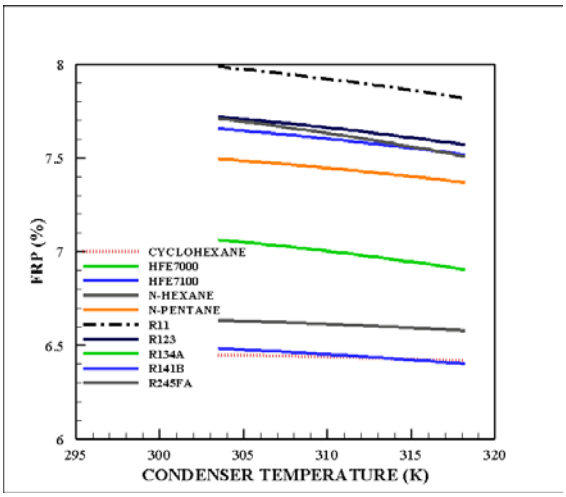

Figure 8. Effect of the condenser's temperature on the fuel reduction percentage.

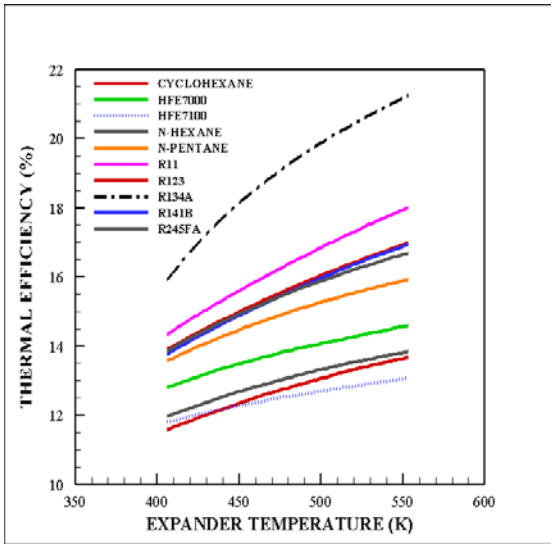

Figure 9. Effect of the expander's temperature on the thermal efficiency.

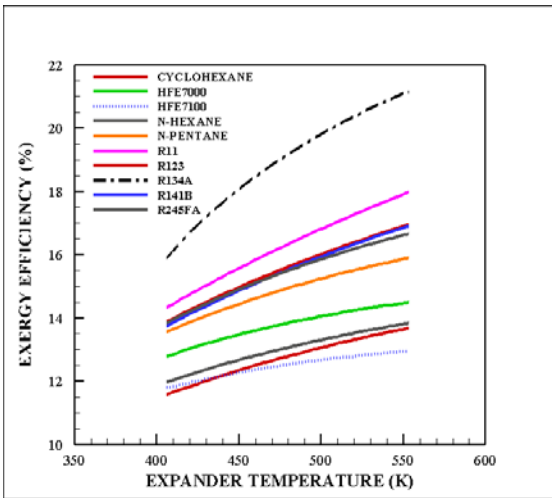

Figure 10. Effect of the expander's temperature on the exergy efficiency.

Figure 11 indicates that with the expander's varying inlet temperatures, HFE7100 and R11 have the highest and lowest total exergy losses, respectively. Although the exergy loss of most of the components decreases by increasing temperature, a remarkable increase in the loss of high-temperature recuperator and evaporator leads to an increase in the total exergy loss.

An increase in the expander's inlet temperature versus FPR is shown in Figure 12. The higher the temperature, the higher the FPR becomes. Since the thermal efficiency of the cycle is fixed, when it is combined with the bottoming ORC, the thermal efficiency of the engine increases. The reason is the increase of the net power of the cycle. According to the graphs, the R134a and HFE7100 have the maximum and minimum reductions, respectively.

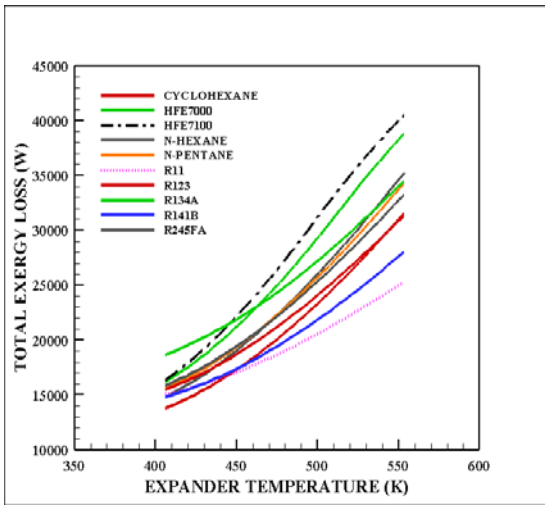

Figure 11. Effect of the expander's temperature on the total exergy loss.

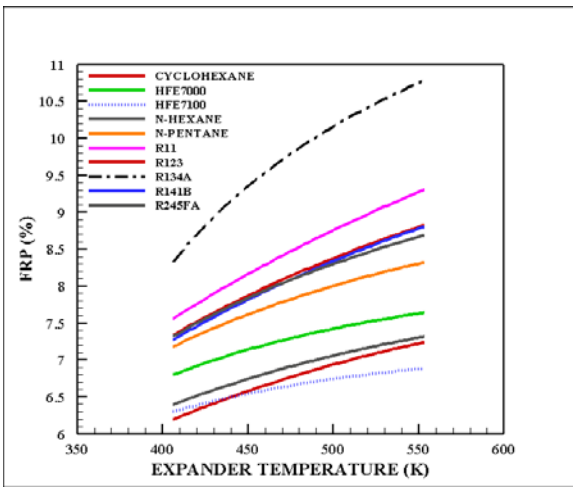

Figure 12. Effect of the expander's temperature on the fuel reduction percentage.

5.3. Effect of the expansion ratio of the expander

Thermal and exergetic efficiencies are plotted versus the expander expansion ratio, as shown in Figures 13 and 14. According to the diagrams, increasing the expansion value leads to increased efficiencies, except for R134a that has an optimum ratio, after which a decrease happens. For all of the working fluids, both expander and pump work increase with the increasing ratio. Therefore, the first and second laws of thermodynamic become more significant. For R134a, up to a definite ratio, both pump and expander work level up. However, after exceeding a specific quantity, the expander work starts decreasing, which leads to a decrease in the net power of the cycle.

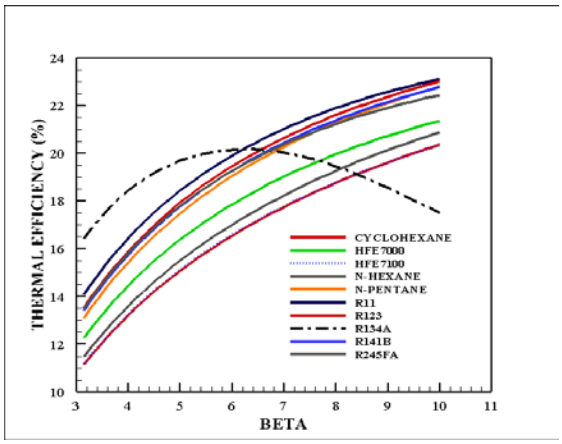

Figure 13. Effect of the expander's expansion ratio on the thermal efficiency.

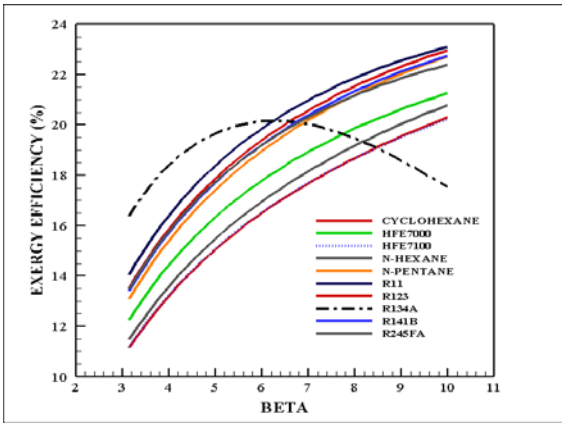

Figure 14. Effect of the expander's expansion ratio on the exergy efficiency.

Since the expander's expansion ratio goes up, the total exergy loss of the cycle increases, which is shown in Figure 15. Although the exergy loss of preheater and recuperators decreases with a rise in the expansion ratio, the exergy loss increases in other components, which is very high in the expander that causes a significant increase in the exergy loss of the system.

Fuel reduction percentage is plotted versus the expander expansion ratio in Figure 16. By increasing the expansion ratio, both pump and expander work level up, resulting in an increase in the FRP of the system. However, R134a treats differently. For this working fluid, there is an optimum ratio at which the FRP of the cycle starts decreasing.

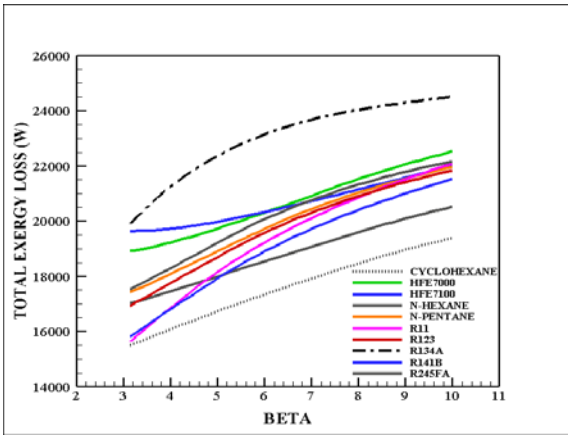

Figure 15. Effect of the expander's expansion ratio on the total exergy loss.

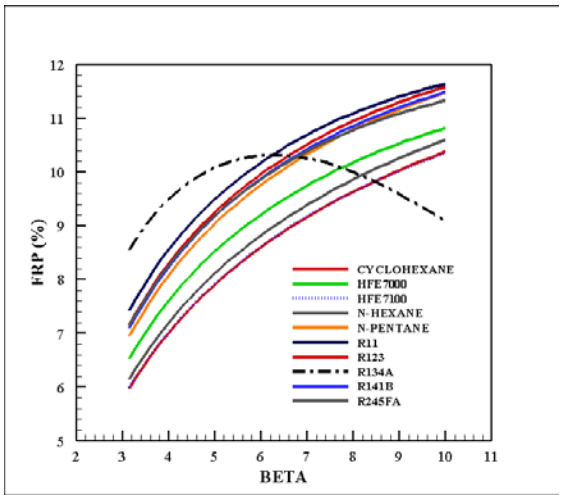

Figure 16. Effect of the expander's expansion ratio on the fuel reduction percentage.

6. CONCLUSIONS

This paper investigates the high-temperature waste heat recovery of a four-cylinder, turbocharged diesel engine combined with a bottoming ORC system, which applies engine exhaust gas for evaporation and jacket cooling water for preheating. The simulation of the performance of different components of the cycle was carried out by applying a mathematical program. Cyclohexane, HFE7000, HFE7100, n-hexane, n-pentane, R11, R123, R134a, R141b, and R245fa were chosen as the working fluids. After conducting a comprehensive thermodynamic analysis of the performance of the system, the following conclusion can be drawn:

1. The efficiencies of the first and second laws decrease as the exhaust temperature increases.
2. Increasing the expansion ratio of the expander, condenser, and expansion temperatures leads to an increase in a significant exergy loss of the system.
3. Condenser temperature rise decreases the fuel percentage and efficiencies of the cycle, while an increase in the expander's temperature increases FRP and thermodynamic efficiencies.
4. There is an optimum expansion ratio at which R134a becomes maximum in FRP and efficiencies, which are important in designing the system.
5. By applying R134a as the working fluid, the maximum net power could be achieved, which was 7.048 kW.
6. In the studied range, the maximum total exergy loss and the exergy destruction factor of the WHR-ORC system were 20.512 kW and 0.006 kW, respectively, in the case of R134a.
7. The maximum amount of engine thermal efficiency belonged to R134a, which provided a 3.78 % increase compared with the engine without bottoming ORC.
8. The energy and exergy efficiencies rose to 17.39 and 17.34 % when the system operated with R134a, which was the maximum.
9. The reduction of fuel consumption was also investigated, which resulted in about a 9 % reduction in fuel consumption.
10. The simulation results made it clear that the best performance was obtained when R134a was applied as the working fluid.

7. ACKNOWLEDGEMENT

The authors would like to specially thank the financial support from Urmia University to carry out this research project.

NOMENCLATURE

C	Specific heat ($kJkg^{-1}K^{-1}$)
$\dot{E}$	Exergy destruction rate (kW)
EDF	Exergy destruction factor
FRP	Fuel reduction percentage
h	Specific enthalpy ($kJ\ kg^{-1}$)
I	Irreversibility
$\dot{m}$	Mass flow rate (kgs^{-1})
ORC	Organic rankine cycle
P	Power
$\dot{Q}$	Heat transfer rate (kW)
S	Specific entropy ($kJkg^{-1}K^{-1}$)
T	Temperature (K)
WHR	Waste heat recovery
$\dot{W}$	Power rate (kW)
Greek symbols	
β	Expansion ratio
η	Efficiency
ψ	Specific flow exergy (kJ)
Subscripts	
0	Reference environment
$1,2,\ldots$	Cycle locations
con	Condenser
D	Destruction
eng	Engine
eva	Evaporator
ex	Exergy
exp	Expander
HP	High pressure
g	Gas
cw	Cooling water
HT	High temperature
in	Inlet
jw	Jacket water
LT	Low temperature
m	Mean
net	Net
out	Outlet
p	Pump
ph	Preheater
r	Recuperator
s	Isentropic process
th	Thermal
tot	Total
wf	Working fluid

REFERENCES

1. Molina-Thierry, D.P. and Flores-Tlacuahuac, A., "Simultaneous optimal design of organic mixtures and Rankine cycles for low-temperature energy recovery", ***Industrial & Engineering Chemistry Research***, Vol. 54, (2014), 3367-3383. (https://doi.org/10.1021/ie503675v).
2. Benvenuto, G., Trucco, A. and Campora, U., "Optimization of waste heat recovery from the exhaust gas of marine diesel engines", ***Proceedings of the Institution of Mechanical Engineers, Part M: Journal of Engineering for Maritime Environment***, Vol. 230, (2016), 83-94. (https://doi.org/10.1177/1475090214533320).
3. Graa Andreasen, J., Meroni, A. and Haglind, F., "A comparison of organic and steam Rankine cycle power systems for waste heat recovery on large", ***Ships Energies***, Vol. 10, (2017), 547-560. (https://doi.org/10.3390/en10040547).
4. Lecompte, S., Oyewunmi, O.A., Markides, C.N., Lazova, M., Kaya, A., Van den Broek, M. and De Paepe, M., "Case study of an Organic Rankine Cycle (ORC) for waste heat recovery from an electric arc furnace (EAF)", ***Energies***, Vol. 10, (2017), 649-662. (https://doi.org/10.3390/en10050649).
5. Shu, G., Yu, G., Tian, H., Wei, H. and Liang, X., "A multi-approach evaluation system (MA-ES) of Organic Rankine Cycle (ORC) used in waste heat utilization", ***Applied Energy***, Vol. 132, (2014), 325-338. (https://doi.org/10.1016/j.apenergy.2014.07.007).
6. Patel, P.S. and Doyle, E.F., "Compounding the truck diesel engine with an Organic Rankine Cycle system", ***SAE Technical Paper 760343***, (1976). (https://doi.org/10.4271/760343).
7. Vaja, I. and Gambarotta, A., "Internal combustion engine (ICE) bottoming with Organic Rankine Cycles", ***Energy***, Vol. 35, (2010), 1084-1093. (https://doi.org/10.1016/j.energy.2009.06.001).
8. Lu, Y.J., Paulroskilly, A., Smallbone, A., Yu, X. and Wang, Y., "Design and parametric study of an Organic Rankine Cycle using a scroll expander for engine waste heat recovery", ***Energy Procedia***, Vol. 105, (2017), 1420-1425. (https://doi.org/10.1016/j.egypro.2017.03.530).
9. Tahani, M., Javan, S. and Biglari, M., "A comprehensive study on waste heat recovery from internal combustion engines using Organic Rankine Cycle", ***Thermal Science***, Vol. 17, (2013), 611-624. (https://doi.org/10.2298/TSCI111219051T).
10. Panesar, A.S., "An innovative Organic Rankine Cycle system for integrated cooling and heat recovery", ***Applied Energy***, Vol. 186, (2013), 396-407. (https://doi.org/10.1016/j.apenergy.2016.03.011).
11. Gequn, S., Hua, T., Haiqiao, W. and Lina, L., "Simulation and thermodynamic analysis of a bottoming Organic Rankine Cycle (ORC) of diesel engine (DE)", ***Energy***, Vol. 5, (2013), 281-290. (https://doi.org/10.1016/j.energy.2012.10.054).
12. Song, S., Zhang, H., Lou, Z., Yang, F., Yang, K., Wang, H., Bei, C., Chang, Y. and Yao, B., "Performance analysis of exhaust waste heat recovery system for stationary CNG engine based on Organic Rankine Cycle", ***Applied Thermal Engineering***, Vol. 76, (2015), 301-309. (https://doi.org/10.1016/j.applthermaleng.2014.11.058).
13. Song, J. and Gu, C.W. "Analysis of ORC (Organic Rankine Cycle) systems with pure hydrocarbons and mixtures of hydrocarbon and retardant for engine waste heat recovery", ***Applied Thermal Engineering***, Vol. 89, (2015), 693-702. (https://doi.org/10.1016/j.applthermaleng.2015.06.055).
14. Shu, G., Li, X., Tian, H., Liang, X., Wei, H. and Wang, X., "Alkanes as working fluids for high-temperature exhaust heat recovery of diesel engine using Organic Rankine Cycle", ***Applied Energy***, Vol. 119, (2014), 204-217. (https://doi.org/10.1016/j.apenergy.2013.12.056).
15. Kim, Y.M., Shin, D.G., Kim, C.G. and Cho, G.B., "Single-loop Organic Rankine Cycle for engine waste heat recovery using both low- and high-temperature heat sources", ***Energy***, Vol. 96, (2016), 482-494. (https://doi.org/10.1016/j.energy.2015.12.092).
16. Klein, S.A., Engineering equation solver version 8.414, professional version, McGraw-Hill, (2009).